Enhancing linear quadratic regulator and proportional-integral linear quadratic regulator controllers for photovoltaic systems

Mohamed Assabaa[1,3], Adel Bouchahed[2,3], Abdellah Draidi[3], Boudjemaa Mehimmedetsi[4], Ahmed Belhani[2]

[1]Laboratoire de Traitement de Signal, Department of Electronics, Faculty of Science and Technology, University of Constantine 1, Constantine, Algeria
[2]Laboratoire Satellites Intelligence Artificielle Cryptographie et Internet des Objets, Department of Electronics, Faculty of Science and Technology, University of Constantine 1, Constantine, Algeria
[3]Electromechanical Department, Institute of Science and Applied Techniques, University of Constantine 1, Constantine, Algeria
[4]Electromechanical Department, Institute of Science and Technology, Abdelhafid Boussouf University Center, Mila, Algeria

Article Info

Article history:

Received Sep 4, 2024
Revised Dec 15, 2024
Accepted Jan 16, 2025

Keywords:

DC-DC boost converter
LQR and LQR-PI corrector
P&O MPPT
Photovoltaic panel PV
PWM control

ABSTRACT

This article introduces the linear quadratic regulator (LQR) control and the hybrid linear quadratic regulator proportional-integral (LQR-PI) control, both applied to a photovoltaic system coupled with a DC-DC boost converter. The converter outputs direct current electrical energy to power direct loads. Two robust control correctors, based on the LQR and LQR-PI methods, are designed to enhance the static and dynamic performance of the PV DC-DC boost system. These controllers aim to minimize oscillations and overshoots while ensuring stability across varying solar conditions, thereby optimizing operation around the maximum power point. The disturb and observe maximum power point tracking (MPPT) technique, integrated with the LQR and LQR-PI controllers, ensures system functionality under disturbances. The novelty of this work lies in the development of a MATLAB control block diagram capable of regulating the reference voltage provided by the perturb and observe (P&O) MPPT algorithm. MATLAB simulations demonstrate the robustness and high performance of the LQR and LQR-PI controllers, validating the efficacy of this boost converter control strategy.

Corresponding Author:

Mohamed Assabaa
Laboratoire de Traitement de Signal, Department of Electronics, Faculty of Science and Technology, University of Constantine 1
Constantine, Algeria
Electromechanical Department, Institute of Science and Applied Techniques, University of Constantine 1
Constantine, Algeria
Email: mohamed.assabaa@umc.edu.dz

1. INTRODUCTION

Photovoltaic (PV) systems are increasingly being adopted as a viable solution for harnessing solar energy, especially in isolated areas where access to centralized electricity networks is unavailable. However, these systems encounter notable challenges due to the irregular availability of sunlight, resulting in variations in voltage, current, and power output. To mitigate these issues, maximum power point tracking (MPPT) techniques are commonly employed to optimize energy capture under fluctuating conditions. Furthermore, advanced control strategies, such as proportional-integral (PI), linear quadratic regulator (LQR), and model predictive control, have been explored to enhance operational stability and overall system performance.

Despite these advancements, PV systems often struggle with inefficiencies, including power oscillations, slow response times, and diminished performance under dynamic environmental factors.

This study aims to address these challenges by enhancing the performance of PV-DC-to-DC boost-converter systems through the implementation of advanced control techniques. A hybrid control approach is developed, combining LQR and proportional-integral (LQR-PI) methods with the perturb and observe (P&O) MPPT algorithm, to achieve improved static and dynamic responses. This approach focuses on minimizing power fluctuations and improving stability during variations in solar irradiance, ensuring efficient and reliable operation. These improvements are particularly vital for regions like the southern Mediterranean, including Algeria, where dependable solar energy solutions are critical for supporting applications such as agriculture and irrigation. The outcomes of this research contribute to advancing PV system control methodologies, fostering greater adoption and optimized use of solar power in practical applications. In the subsequent paragraphs, a compilation of pertinent literature highlighting these research efforts will be presented.

The study presents an analysis, design, and implementation of nonlinear controllers tailored for the fundamental negative super lift Luo-converter, a direct current-direct current (DC-to-DC) converter featuring advanced topology. To enhance dynamic load voltage analysis and current control within the coil of the fundamental negative super lift Luo-converter (FNSLLC), a linear quadratic regulator (LQR) and a fuzzy logic controller are devised. The LQR controller governs the current passing through the coil within the inner servo loop, while the FLC controller controls the load voltage in the outer voltage loop. The efficacy of employing LQR alongside FLC in optimizing FNSLLC performance is validated through various run tests conducted using MATLAB/Simulink and a programmable prototype on board (FPGA) [1].

An LQR is employed to control a hybrid power system comprising an ultracapacitor for energy storage and a wind power system. The primary objective of this control scheme is to regulate the direct current bus voltage to a predefined level while maximizing the extraction of available wind energy. Through extensive testing across various scenarios, encompassing both simulations and experiments, the efficacy of the proposed LQR controllers is demonstrated. They exhibit robustness by accurately tracking voltage and current references, swiftly restoring the system to its nominal operating state under diverse conditions, including fluctuations in wind speed and load demand [2].

A combination of a LQR and a Kalman filter (KF) is employed to regulate the output parameters of a buck-boost converter and mitigate disturbances. This control methodology is applied in conjunction with a solar panel system. The outcomes of the study indicate that the proposed controller effectively manages the adjustment of output quantities of the DC-to-DC converter and facilitates accurate tracking of the maximum power point [3]. The study introduces a novel control technique utilizing the LQR method in single-phase grid-connected photovoltaic systems. Compared to the backstepping method, the LQR technique demonstrates greater resilience to sudden changes and disturbances, resulting in reduced overshoot. Simulation outcomes underscore the robustness of the LQR control across diverse weather conditions, affirming its effectiveness in photovoltaic system regulation [4]. A design of X DC-to-DC converter incorporating an optimal LQR controller along with integrated gain action results in high stability across different output characteristics of the DC-DC converter [5]. A robust control strategy for a DC-DC boost converter, utilizing a LQR and leveraging the potential of linear matrix inequalities (LMIs), guarantees high stability across various simulation results [6].

In the system, a P&O algorithm-based MPPT technique serves as an external loop controller, managing the reference voltage required by the LQR controller. This setup, compared to the PI controller, demonstrates superior performance and robustness. Overall, the system effectively tracks the maximum power point, yielding satisfactory results [7].

To reach average power and stand-alone operation through the integration of a DC-to-DC boost-converter into fuel cells (FC), a LQR is developed for controlling the power converter's parameters. However, in practical applications, the classic LQR may introduce an offset in the output voltage due to the effective series resistance (ESR) of the output capacitor. To address this issue and enhance system performance, two modifications are proposed: the m-LQR controller, which minimizes the impact of ESR, and the M-LQR controller, which regulates the inductor current. Both modifications yield superior results compared to the classic LQR controller [8]. In another application aimed at enhancing power supply quality and controlling power flow between a PV system and a non-linear load, a LQR is employed to mitigate power quality degradation in the grid, especially during climate variations. The effectiveness of this approach is validated using the MATLAB/Simulink environment [9].

In a PV-wind hybrid water pumping system, the energy sources are linked via a multi-input DC-to-DC converter, with its output directly connected to a DC motor pump, bypassing the need for a battery bank. To enhance system performance, a linear quadratic Gaussian (LQG) controller with loop transfer recover regulator (LQG/LTR), in combination with a regulator LQR, is implemented. This configuration enables the system to achieve high static and dynamic performance. Simulation results demonstrate the robustness of the controller when applied to the system [10]. In a separate study, a nonlinear observer is developed based on both sliding mode controller (SMC) and extended Kalman filter (EKF). These observers utilize a process model to facilitate the operation of a system comprising a DC-to-DC boost-converter integrated with a fuel cell system. The integrated controlled system operates without voltage drop, maintaining stability compared to a traditional PI controller. The Findings are validated using the MATLAB/Simulink simulations [11].

This article explores two distinct control techniques utilized for a DC-to-DC boost photovoltaic-converter system. The first technique combines a P&O-MPPT with linear quadratic regulator control. The second technique integrates the P&O-MPPT technique with proportional-integral linear quadratic regulator control. Both approaches aim to regulate the voltage and current output of the converter directly. However, the performance of these output characteristics varies between the two methods.

Our contribution involves the design of an MPPT approach using the P&O method, combined with LQR-PI control. We achieve this by integrating a proportional integral (PI) corrector into a voltage servo loop, where the reference voltage is derived from a mathematical equation. This enhancement enables the system to operate with reduced oscillations and disturbances during changes in illumination compared to conventional LQR control methods. We conducted simulations of these control techniques using the MATLAB environment, varying irradiances applied to the DC-to-DC boost photovoltaic system to assess their performance.

Table 1 is a nomenclature table that defines the various acronyms and abbreviations used throughout this article. It ensures clarity by providing concise explanations of key terms and symbols. This reference aids in understanding the concepts and control strategies discussed.

Table 1. Nomenclature

Abbreviation	Meaning	Abbreviation	Meaning
PV	Solar panel	P_{pv}	PV power (watt)
FNSLLC	Fundamental negative super lift Luo-converter	S_W	MOSFET switch
FLC	Fuzzy logic controller	N_p	Parallels modules
FPGA	Electronic programming card	I_{sat}	Saturation of solar cells in dark current (A)
CC	Continuous-continuous	R_{se}	Resistance in series (Ω)
DC	Direct current	R_{pe}	Parallel resistance (Ω)
KF	Kalman filter	N_s	Series modules
LMIs	Linear matrix inequalities	I_{0r}	The current of reverse saturation
MPPT	Maximum power point tracking	T	Actual temperature
FC	Fuel cell	T_0	Cell's reference temperature (◦C)
P&O	Perturb and observe	q	Electron charge (C)
ESR	Effective series resistance	E_G	Tape space (W/m2)
m-LQR	Modifications-linear quadratic regulator	K	Boltzmann's constant (J/K)
M-LQR	Modifications-linear quadratic regulator	a	Ideality factor
MIC	Multi-input DC-DC converter	K_i	Temperature coefficient
LQG/LTR	Linear quadratic Gaussian control improved with loop transfer recovery	I_{cc}	short circuit current
SMC	Sliding mode controller	G, G_r	Solar and reference radiation (W/m^2)
EKF	Extended Kalman filter	I_{ph}	Photocurrent (A)
PI	Proportional integral controller	L	Inductor (H)
P&O MPPT	Perturb and observe maximum power point tracking	C_{in}	Capacitor at boost input (µF)
LQR-PI	Linear quadratic regulator–proportional integral	u	switch control signal
LQR	Linear quadratic regulator	K_P	Proportional Gain
DC-DC	Direct current-direct current	K_I	integral gain
PWM	Pulse width modulation	V_{dc}	DC bus voltage (V)
$\boldsymbol{V_{pv}}$	Photovoltaic panel output voltage (V)	I_{dc}	DC bus current (A)
$\boldsymbol{i_{pv}}$	Photovoltaic panel output current (A)	R	Load resistance (Ω)
$\boldsymbol{D}$	Diode	C_{out}	boost output capacitor (μF)

2. SYSTEM DESCRIPTION

The system presented in this work is comprised of a photovoltaic panel connected to a DC-to-DC boost converter, supplying power to a resistive load, as illustrated in Figure 1. The photovoltaic generator produces voltage and current, which are fed into the terminals of the DC-to-DC boost-converter. The converter then elevates the voltage from the photovoltaic generator to an suitable level based on the input supply voltage's amplitude. The controllers utilized in this study are designed to operate the PV-boost system at its MPPT, thereby enhancing the static performance of the photovoltaic system coupled with a boost DC-to-DC converter.

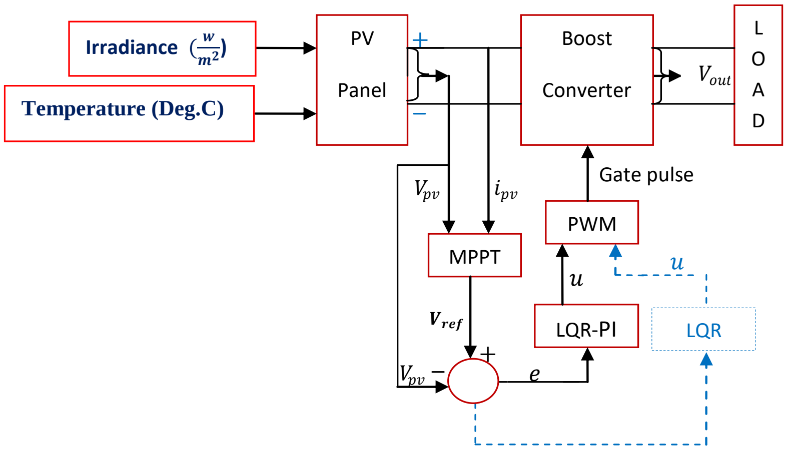

Figure 1. Photovoltaic system connected to a DC-to-DC boost-converter

2.1. Mathematical model of photovoltaic system and boost-converter

Figure 2 presents the application of two different control strategies for a DC-DC boost converter. These techniques are implemented within a photovoltaic system. The figure highlights the distinct approaches and their integration into the system.

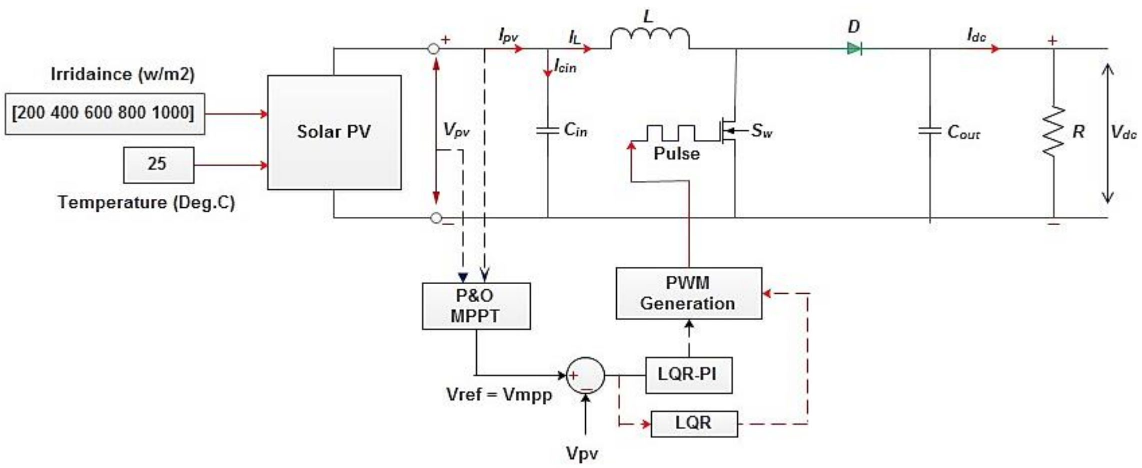

Figure 2. Structural diagram of the LQR and LQR-PI control utilized for the boost converter associated with a PV panel

From the diagram in Figure 2, the equations governing the behavior of the photovoltaic (PV) panel and boost converter are derived. These equations capture the system's dynamics and interactions. They form the basis for analyzing the performance of the system as follow: The mathematical model governing the operation of the photovoltaic system, as proposed by several researchers [12]–[20], can be expressed as (1) to (3):

$$I_{pv(} = N_p I_{ph} - N_p I_{sat}\left[exp\left(\frac{q(V_{pv}+\frac{N_s}{N_p}I_{pv}R_{se})}{a\,K\,T\,n_s}\right)-1\right]-\frac{V_{pv}+\frac{N_s}{N_p}I_{pv}R_{se}}{\frac{N_s}{N_{sh}}R_{pe}} \tag{1}$$

with

$$I_{sat} = I_{satr}\left(\frac{T}{T_0}\right)^3 exp\left[\frac{qE_G}{K\,a}\left[\frac{1}{(273+25)}-\frac{1}{T}\right]\right] \tag{2}$$

$$I_{ph} = [I_{cc} + K_i(T - (273 + 25)] \frac{G}{G_r} \tag{3}$$

The mathematical expressions that describe the functioning of the boost-converter are detailed below [21]–[26]:
when the S_w is in the closed position and the diode *D* is reverse-biased, during the interval $t \in [\mathrm{t}_0, \mathrm{t}_0 + \mathrm{dT}\ ]$, the following equations apply:

$$L\frac{di_l}{dt} = V_{PV} \tag{4}$$

$$C\frac{dv_{dc}}{dt} = -\frac{v_{dc}}{R} \tag{5}$$

when the S_w is in the open state and the diode *D* is forward-biased, during the interval $t \in [\mathrm{t}_0 + \mathrm{dT}, \mathrm{t}_0 + \mathrm{T}\ ]$, the following equations are obtained:

$$L\frac{di_l}{dt} = V_{PV} - V_{dc} \tag{6}$$

$$C\frac{dv_{dc}}{dt} = i_l - \frac{v_{dc}}{R} \tag{7}$$

The dynamic model of the boost-converter under continuous conduction operation are presented as (8) and (9).

$$L\frac{di_L}{dt} = V_{PV} - V_{dc}(1-u) \tag{8}$$

$$C\frac{dV_{dc}}{dt} = i_L\,(1-u) - \frac{V_{dc}}{R} \tag{9}$$

with *u* define the control signal of IGBT. We set: $x_1 = i_L$ and $x_2 = V_{dc}$ then (8) and (9) become:

$$\dot{x}_1 = \frac{V_{PV}}{L} - \frac{x_2(1-u)}{L} \tag{10}$$

$$\dot{x}_2 = \frac{x_1\,(1-u)}{C} - \frac{x_2}{RC} \tag{11}$$

The complete system parameters consist of the coil inductance *L* [H], the capacitor capacitance *C* [F] and the load resistance *R* [Ω]. The state variables are defined by the coil current and the capacitor voltage. The control signal uuu takes values from the set {0,1}, representing the state of the switch S_w: 0 for open and 1 for closed. This control signal can be replaced by its average value over a chopping period, denoted as *d*, which represents the duty cycle $d = T_{on}/T_s$, where T_{on} is the conduction time and T_s is the chopping period.

The set of equations given by (10) and (11) can be expressed in a state-space representation as (12) and (13).

$$\begin{bmatrix} \dot{x}_1 \\ \dot{x}_2 \end{bmatrix} = \begin{bmatrix} 0 & -\frac{(1-d)}{L} \\ \frac{(1-d)}{C} & -\frac{1}{RC} \end{bmatrix} \begin{bmatrix} x_1 \\ x_2 \end{bmatrix} + \begin{bmatrix} \frac{1}{L} \\ 0 \end{bmatrix} V_{pv} \tag{12}$$

$$y = [0 \quad 1] \begin{bmatrix} i_L \\ V_{dc} \end{bmatrix} \tag{13}$$

The system is linearized around an equilibrium point with (14).

$$\begin{cases} \dot{x} = 0 \\ 0 = AX + BU \\ X = -A^{-1}BU \\ x = X + \tilde{x} \\ d = D + \tilde{d} \\ i_L = I_L + \tilde{i_L} \end{cases} \tag{14}$$

From (12) and (14), we can derive the linear model of the system [7], [27], [28].

$$\begin{bmatrix} \dot{\tilde{i}}_L \\ \dot{\tilde{V}}_{dc} \end{bmatrix} = \begin{bmatrix} 0 & -\frac{(1-D)}{L} \\ \frac{(1-D)}{C} & -\frac{1}{RC} \end{bmatrix} \begin{bmatrix} \tilde{i}_L \\ \tilde{V}_{dc} \end{bmatrix} + \begin{bmatrix} \frac{V_{dc}}{L} \\ -\frac{1}{C} \end{bmatrix} \tilde{d} + \begin{bmatrix} \frac{1}{L} \\ 0 \end{bmatrix} \widetilde{V_{pv}} \quad (15)$$

$$\tilde{y} = \begin{bmatrix} 0 & 1 \\ 1 & 0 \end{bmatrix} \begin{bmatrix} \tilde{i}_L \\ \tilde{V}_{dc} \end{bmatrix} \quad (16)$$

2.2. Constitution of the MPPT perturb and observe algorithm

The P&O method for MPPT is analyzed in numerous studies, such as those cited in [29]–[34]. This technique uses the voltage and current outputs from the PV system as key variables. By utilizing these variables, the power at the current time $p(t)$ and at the previous time step $p(t-1)$ can be computed. Figure 3 illustrates the P&O technique, which is designed to identify the maximum power point.

Figure 3 depicts a PV system connected to a boost converter, which is regulated using the P&O MPPT algorithm. This method is compared against a ramp-shaped carrier signal to produce pulse-width modulation (PWM). The PV panel's behavior is modeled in MATLAB Simulink using (1)-(3), which account for parameters such as variable irradiance, temperature, and the arrangement of cells in series and parallel. These factors collectively enhance the voltage and current output of the PV module. The boost converter's output voltage is subsequently supplied to a resistive load.

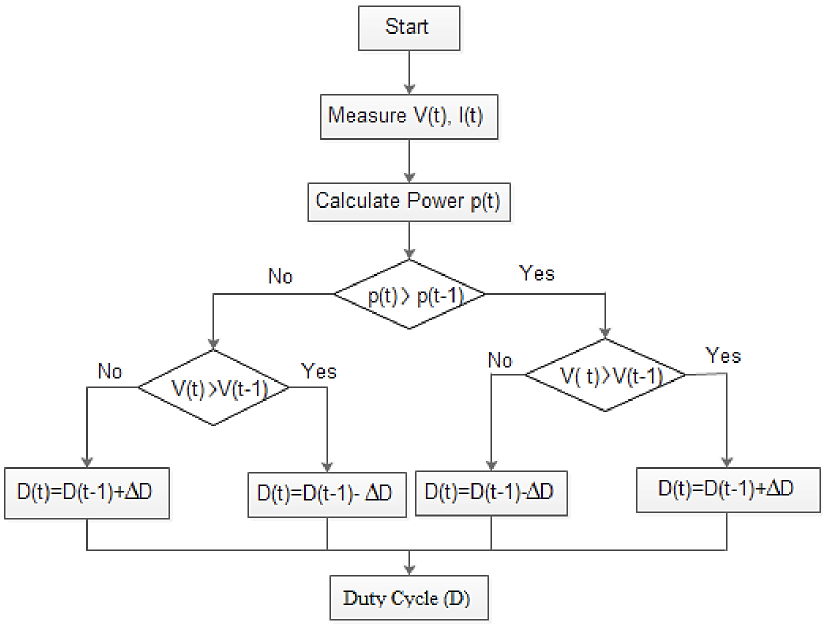

Figure 3. P&O algorithm

3. DESIGN OF THE LQR AND LQR-PI CONTROL LAW

Using the equations governing the boost-converter, we can develop a control law utilizing the LQR method and a hybrid LQR-PI control, expressed through state equations:

$$\begin{aligned} \dot{x} &= Ax(t) + Bu(t) \\ y &= Cx(t) \end{aligned} \quad (17)$$

with: x, u, y, A, B and C are respectively: state vector, input vector, output vector, state matrix, control matrix, and the output matrix.

To achieve high static and dynamic performance in controlling the boost converter, we represent the system described by state (17) in the configuration of a closed-loop system as showed in Figure 4:

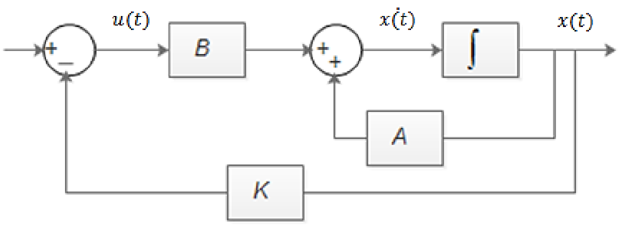

Figure 4. The main configuration of the LQR corrector

In which K represent the gain matrix, and control vector is given by (18):

$$u(t) = -K.x(t) \tag{18}$$

To enhance the efficiency of the boost-converter control, we employ the infinite horizon L-Q-R theory, using the following criterion [35]–[38]:

$$J = \frac{1}{2}\int_0^{\infty}(x^T(t)Qx(t) + u^T(t)Ru(t))dt \tag{19}$$

when the control is time-invariant and linear, the control law simplifies to a constant state feedback, where K is derived from (18), and P is defined in the Riccati equation in algebraic form:

$$P(t)A + A^TP(t) - P(t)BR^{-1}B^TP(t) + Q = 0 \tag{20}$$

with $Q \geq 0$ and $R > 0$ exhibit symmetry in their matrix form.

For the stabilization of our system, state feedback control theory is applied with an optimal control approach, which induces a closed-loop system:

$$u(t) = -R^{-1}B^TPx(t) \tag{21}$$

where The matrix P, satisfying the Riccati algebraic equation, remains asymptotically stable under the following conditions: the pair $\{A, B\}$ satisfies the controllability condition, while the pair $\{A, \sqrt{Q}\}$ is detectable. Additionally, P is positive if and only if the pair $\{A, \sqrt{Q}\}$ is fully visible. Accordingly, full set of eigenvalues associated with the matrix $[A - BR^{-1}B^TP]$ will have negative real parts.

Figure 5 illustrates the L-Q-R and L-Q-R-PI control laws, with the PI corrector expressed as (22)

$$u(t) = K_pe(t) + K_I\int_0^t e(t)dt \tag{22}$$

where K_p is the proportional gain and K_I is the integral gain.

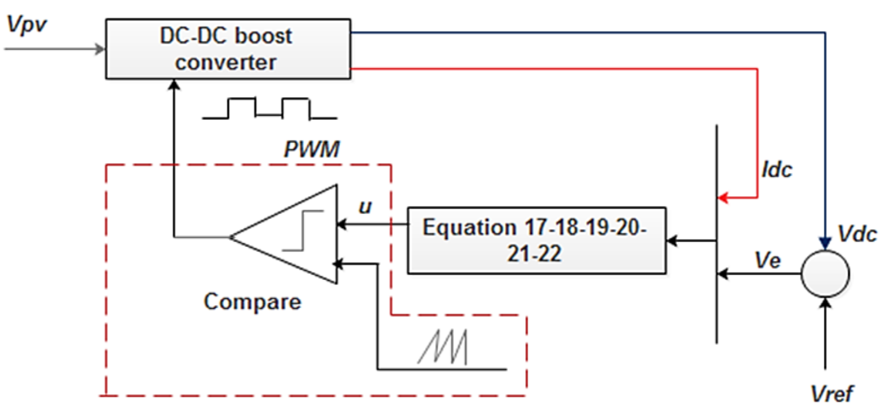

Figure 5. Block diagram of the LQR and LQR-PI control

4. RESULTS AND DISCUSSION

The mathematical models for the PV system and DC-to-DC boost-converter are presented in a block diagram format. The PV system operates under variable illumination of [200 to 1000] W/m^2 and a temperature of 25 °C. These models capture the system's behavior and performance under these conditions.

To generate different results, the DC-to-DC boost-converter parameters are specified in Table 2. The study highlights the benefits of LQR and LQR-PI control strategies in improving the performance of a PV-powered DC-to-DC boost-converter. These techniques are shown to enhance system operation under changing illumination levels. The results demonstrate significant performance improvements in such dynamic conditions.

Figure 6 illustrates how the voltage, current, and power at the output of the PV panel vary with changes in illumination and temperature. Specifically, at an illumination level of 1000 W/m², the PV power P_{pv} is 147 Watts. This power decreases as illumination drops, reaching 35 Watts at 200 W/m². The voltage characteristic, as a function of time, ranges between 34.5 and 38.3 Volts, depending on the applied illumination. Additionally, the shape of the I_{pv} current waveform changes with variations in illumination; for G = 1000 W/m², the I_{pv} current is 4.2 Amperes.

Figure 7 shows the V_{dc} voltages applied across the resistive load, controlled by two different techniques. The blue curve represents the V_{dc} voltage achieved with the LQR-PI control method, while the red curve corresponds to the LQR technique. The LQR-PI method demonstrates superior response time and reduced overshoot compared to the LQR method. The V_{dc} voltage using the L-Q-R-PI technique effectively tracks changes in illumination, reaching up to 55 Volts for an illumination of 1000 W/m².

Figure 8 presents the current characteristics. The I_{dc} current controlled by the LQR-PI technique exhibits better response time, stability, and minimal overshoot compared to the LQR method. The I_{dc} current also accurately follows changes in illumination, reaching up to 7.8 Amperes for an illumination of 1000 W/m².

Figure 9 illustrates the variation in power delivered at the output of the DC-to-DC boost-converter. The power closely follows changes in illumination applied to the PV system. The blue curve represents the power achieved using the LQR-PI method, which demonstrates superior response time and reduced overshoot compared to the LQR method. With the LQR-PI technique, the maximum direct current power P_{dc} reaches 430 W for an illumination of 1000 W/m², whereas the LQR method achieves a maximum of 400 W.

Figure 10 displays the pulses generated by the PWM technique applied to the MOSFET. The MATLAB simulation results across the various figures indicate the robustness and stability of the L-Q-R-PI control compared to the LQR control technique. The LQR-PI method delivers more stable performance with fewer oscillations, overshoots, and disturbances across the illumination range from 200 to 1000 W/m².

Table 2. Estimated specifications of the DC-to-DC boost converter

Parameters	Estimated parameters
DC voltage at the input $\boldsymbol{V_{PV}}$	$[34.5 - 38.3]V$
Frequency of switching $\boldsymbol{fs}$	20 kHz
Load resistor $\boldsymbol{R}$	12 Ω
Boost converter Inductor $\boldsymbol{L}$	0.01H
Boost converter Capacitor $\boldsymbol{C_{in}} = \boldsymbol{C_{out}}$	0.0000299 F
Output DC voltage $\boldsymbol{V_{dc}}$	$[50 - 55]V$
$\boldsymbol{K_p}$	0.02
$\boldsymbol{K_I}$	0.00010

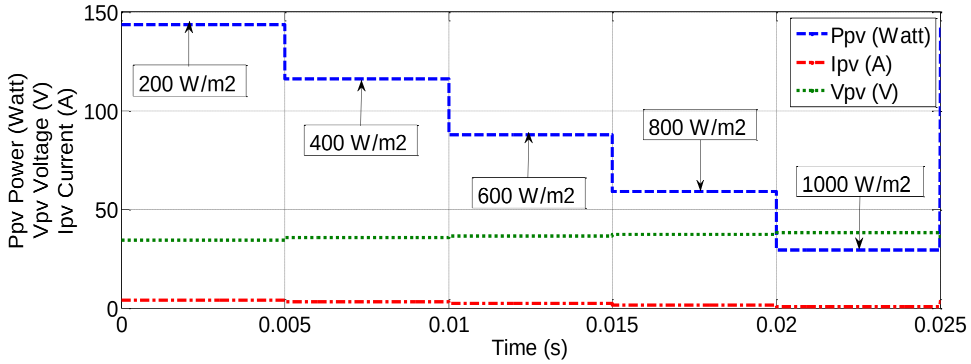

Figure 6. Photovoltaic panel characteristics when changing illumination

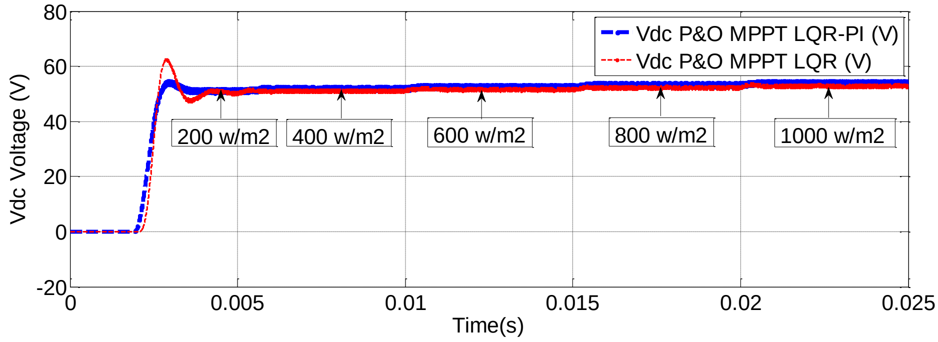

Figure 7. Voltage characteristics for different control techniques when changing illumination

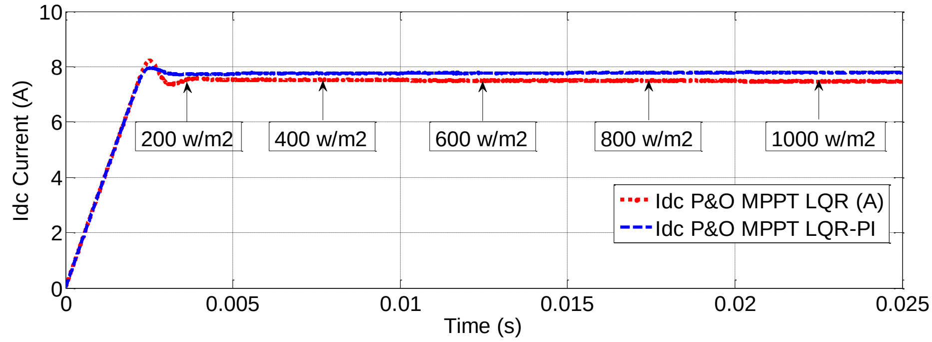

Figure 8. Current characteristics for different control techniques when changing illumination

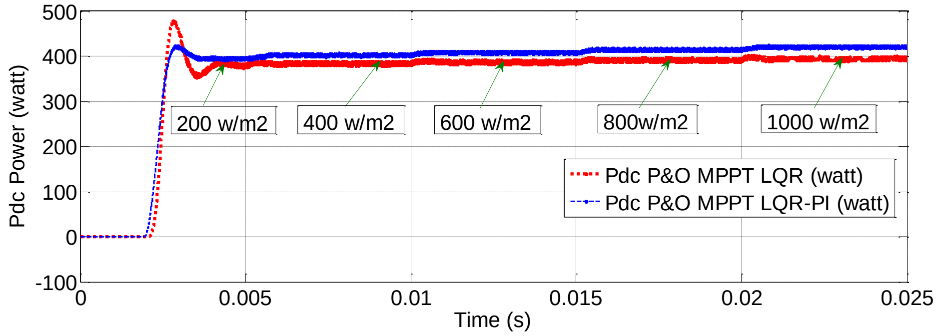

Figure 9. Boost converter output power characteristics for different control techniques when changing illumination

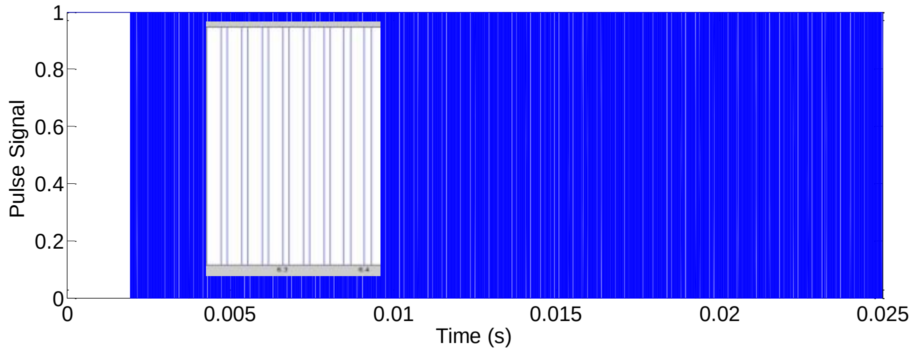

Figure 10. PWM control signal

The results confirm that the LQR-PI control technique significantly outperforms the conventional LQR method in enhancing dynamic performance, power conversion efficiency, and system stability. Specifically, LQR-PI achieves faster response times and minimizes overshoot, ensuring stable and efficient operation under varying illumination conditions. Additionally, the higher output power achieved with LQR-PI control demonstrates its effectiveness in maximizing energy extraction from the PV system. Furthermore, the reduced oscillations and improved tracking of voltage and current highlight the ability of LQR-PI to better handle the nonlinear and dynamic behavior of PV systems, making it a robust solution for improving overall system performance.

5. CONCLUSION

The study highlights the advantages of LQR-PI control in improving the performance of PV-powered DC-to-DC boost-converters, particularly in terms of response time, stability, and power output. In order to improve the static and dynamic performances of the PV-DC-to-DC boost-converter system, the LQR-PI control and the LQR control play a significant role in removing oscillations and fluctuations in the system's various properties of the system especially when changing the illumination. These two previously mentioned techniques are associated with the P&O-MPPT technique.

The LQR-PI control algorithm combined with the P&O-MPPT algorithm provides robust and high-performance operation for the PV-boost system in response to changes in irradiance. It outperforms the LQR control strategy, which experiences some oscillations and overshoots during illumination changes. Simulation results obtained in the MATLAB environment validate the effectiveness and robustness of both control techniques when applied to the photovoltaic system DC-to-DC boost-converter. While the findings confirm the robustness and efficacy of the proposed method, further experimental validation and broader comparisons are necessary to generalize these results to real-world systems.

FUNDING INFORMATION

Authors state no funding involved.

AUTHOR CONTRIBUTIONS STATEMENT

This journal uses the Contributor Roles Taxonomy (CRediT) to recognize individual author contributions, reduce authorship disputes, and facilitate collaboration.

Name of Author	C	M	So	Va	Fo	I	R	D	O	E	Vi	Su	P	Fu
Mohamed Assabaa	✓	✓	✓	✓	✓	✓		✓	✓	✓	✓		✓	✓
Adel Bouchahed	✓	✓	✓	✓	✓	✓		✓	✓	✓	✓			✓
Abdellah Draidi	✓	✓	✓	✓	✓	✓		✓	✓	✓	✓	✓	✓	✓
Boudjemaa Mehimmedetsi			✓	✓	✓		✓					✓		
Ahmed Belhani				✓	✓	✓	✓			✓		✓		

C : **C**onceptualization
M : **M**ethodology
So : **So**ftware
Va : **Va**lidation
Fo : **Fo**rmal analysis
I : **I**nvestigation
R : **R**esources
D : **D**ata Curation
O : Writing - **O**riginal Draft
E : Writing - Review & **E**diting
Vi : **Vi**sualization
Su : **Su**pervision
P : **P**roject administration
Fu : **Fu**nding acquisition

CONFLICT OF INTEREST STATEMENT

Authors state no conflict of interest.

DATA AVAILABILITY

The authors confirm that the data supporting the findings of this study are available within the article.

REFERENCES

[1] K. R. Kumar, N. Arunkumar, and T. S. Sivakumaran, "Implementation of non-linear controller for contemporary DC-DC converter," *International Journal on Electrical Engineering and Informatics*, vol. 11, no. 4, pp. 622–637, Dec. 2019, doi: 10.15676/ijeei.2019.11.4.1.

[2] M. A. Abdullah, A. Q. Al-Shetwi, M. Mansor, M. A. Hannan, C. W. Tan, and A. H. M. Yatim, "Linear quadratic regulator controllers for regulation of the dc-bus voltage in a hybrid energy system: Modeling, design and experimental validation," *Sustainable Energy Technologies and Assessments*, vol. 50, Mar. 2022, doi: 10.1016/j.seta.2021.101880.

[3] D. Quezada, C. Beltrán, J. Rohten, N. Risso, V. Esparza, and M. Rivera, "Linear quadratic control design for a buck-boost power converter supplied by a solar array," in *2021 IEEE International Conference on Automation/XXIV Congress of the Chilean Association of Automatic Control (ICA-ACCA)*, Mar. 2021, pp. 1–6, doi: 10.1109/ICAACCA51523.2021.9465328.

[4] A. Mukhatov, N. G. M. Thao, and T. D. Do, "Linear quadratic regulator and fuzzy control for grid-connected photovoltaic systems," *Energies*, vol. 15, no. 4, Feb. 2022, doi: 10.3390/en15041286.

[5] N. H. Abbas, A. Falah, and A. Algamluoli, "Designing an integral LQR controller for DC-DC X-converter based on enhanced shuffled frogleaping optimization algorithm," *Journal of Electrical Systems*, vol. 16, no. 2, pp. 152–170, 2020.

[6] N. Aouani and C. Olalla, "Robust LQR control for PWM converters with parameter-dependent lyapunov functions," *Applied Sciences*, vol. 10, no. 21, Oct. 2020, doi: 10.3390/app10217534.

[7] A. Brahimi, D. Kerdoun, and A. Boumassata, "Boost converter control using LQR and P&O technique for maximum power point tracking," in *2022 19th International Multi-Conference on Systems, Signals & Devices (SSD)*, May 2022, pp. 1998–2003, doi: 10.1109/SSD54932.2022.9955798.

[8] N. Agrawal, S. Samanta, and S. Ghosh, "Modified LQR technique for fuel-cell-integrated boost converter," *IEEE Transactions on Industrial Electronics*, vol. 68, no. 7, pp. 5887–5896, Jul. 2021, doi: 10.1109/TIE.2020.3000096.

[9] R. Vinifa, A. Kavitha, and A. Immanuel Selwynraj, "Control of power in the grid integrated solar photovoltaic system using linear quadratic regulator," *Materials Today: Proceedings*, vol. 45, pp. 981–985, 2021, doi: 10.1016/j.matpr.2020.03.045.

[10] A. de O. Ferreira, A. U. Brito, M. A. B. Galhardo, L. Ferreira, and W. N. Macêdo, "Modeling, control and simulation of a small photovoltaic-wind water pumping system without battery bank," *Computers & Electrical Engineering*, vol. 84, Jun. 2020, doi: 10.1016/j.compeleceng.2020.106619.

[11] K. Sankar, G. Saravanakumar, and A. K. Jana, "Nonlinear multivariable control of an integrated PEM fuel cell system with a DC-DC boost converter," *Chemical Engineering Research and Design*, vol. 167, pp. 141–156, Mar. 2021, doi: 10.1016/j.cherd.2021.01.011.

[12] R. Celikel, M. Yilmaz, and A. Gundogdu, "A voltage scanning-based MPPT method for PV power systems under complex partial shading conditions," *Renewable Energy*, vol. 184, pp. 361–373, Jan. 2022, doi: 10.1016/j.renene.2021.11.098.

[13] M. Jiang, M. Ghahremani, S. Dadfar, H. Chi, Y. N. Abdallah, and N. Furukawa, "A novel combinatorial hybrid SFL–PS algorithm based neural network with perturb and observe for the MPPT controller of a hybrid PV-storage system," *Control Engineering Practice*, vol. 114, Sep. 2021, doi: 10.1016/j.conengprac.2021.104880.

[14] A. I. M. Ali and H. R. A. Mohamed, "Improved P&O MPPT algorithm with efficient open-circuit voltage estimation for two-stage grid-integrated PV system under realistic solar radiation," *International Journal of Electrical Power & Energy Systems*, vol. 137, May 2022, doi: 10.1016/j.ijepes.2021.107805.

[15] U. Yilmaz, A. Kircay, and S. Borekci, "PV system fuzzy logic MPPT method and PI control as a charge controller," *Renewable and Sustainable Energy Reviews*, vol. 81, pp. 994–1001, Jan. 2018, doi: 10.1016/j.rser.2017.08.048.

[16] A. Borni *et al.*, "Optimized MPPT controllers using GA for grid connected photovoltaic systems, comparative study," *Energy Procedia*, vol. 119, pp. 278–296, Jul. 2017, doi: 10.1016/j.egypro.2017.07.084.

[17] K. Latha Shenoy, C. G. Nayak, and R. P. Mandi, "MPPT enabled SPWM based bipolar VSI design in photovoltaic applications," *Materials Today: Proceedings*, vol. 5, no. 1, pp. 1372–1378, 2018, doi: 10.1016/j.matpr.2017.11.223.

[18] Kitmo, R. Djidimbélé, D. K. Kidmo, G. B. Tchaya, and N. Djongyang, "Optimization of the power flow of photovoltaic generators in electrical networks by MPPT algorithm and parallel active filters," *Energy Reports*, vol. 7, pp. 491–505, Nov. 2021, doi: 10.1016/j.egyr.2021.07.103.

[19] K. Chigane and M. Ouassaid, "Sliding mode control for a transformerless single-phase grid-connected photovoltaic system," in *2017 International Renewable and Sustainable Energy Conference (IRSEC)*, Dec. 2017, pp. 1–6, doi: 10.1109/IRSEC.2017.8477301.

[20] E. M. Ahmed, H. Norouzi, S. Alkhalaf, Z. M. Ali, S. Dadfar, and N. Furukawa, "Enhancement of MPPT controller in PV-BES system using incremental conductance along with hybrid crow-pattern search approach based ANFIS under different environmental conditions," *Sustainable Energy Technologies and Assessments*, vol. 50, Mar. 2022, doi: 10.1016/j.seta.2021.101812.

[21] K. Wang, D. Liu, and L. Wang, "The implementation of synergetic control for a DC-DC buck-boost converter," *Procedia Computer Science*, vol. 199, pp. 900–907, 2022, doi: 10.1016/j.procs.2022.01.113.

[22] T. K. Nizami and A. Chakravarty, "Neural network integrated adaptive backstepping control of DC-DC boost converter," *IFAC-PapersOnLine*, vol. 53, no. 1, pp. 549–554, 2020, doi: 10.1016/j.ifacol.2020.06.092.

[23] T. T. Sarkar and C. Mahanta, "Estimation based sliding mode control of DC-DC boost converters," *IFAC-PapersOnLine*, vol. 55, no. 1, pp. 467–472, 2022, doi: 10.1016/j.ifacol.2022.04.077.

[24] A. Sarikhani, B. Allahverdinejad, M. Hamzeh, and E. Afjei, "A continuous input and output current quadratic buck-boost converter with positive output voltage for photovoltaic applications," *Solar Energy*, vol. 188, pp. 19–27, Aug. 2019, doi: 10.1016/j.solener.2019.05.025.

[25] K. Kumar, R. Tiwari, P. V. Varaprasad, C. Babu, and K. J. Reddy, "Performance evaluation of fuel cell fed electric vehicle system with reconfigured quadratic boost converter," *International Journal of Hydrogen Energy*, vol. 46, no. 11, pp. 8167–8178, Feb. 2021, doi: 10.1016/j.ijhydene.2020.11.272.

[26] M. Iqbal, A. Benmouna, F. Eltoumi, F. Claude, M. Becherif, and H. S. Ramadan, "Cooperative operation of parallel connected boost converters for low voltage-high power applications: An experimental approach," *Energy Procedia*, vol. 162, pp. 349–358, Apr. 2019, doi: 10.1016/j.egypro.2019.04.036.

[27] H. Mishra and S. Ray, "Comprehensive small signal modeling of the DC/DC converters with CDM controller design," in *2020 First International Conference on Power, Control and Computing Technologies (ICPC2T)*, Jan. 2020, pp. 176–181, doi: 10.1109/ICPC2T48082.2020.9071508.

[28] M. Appikonda and K. Dhanalakshmi, "Small-signal modelling and control of a high voltage gain dual input boost DC-DC converter," in *2018 8th IEEE India International Conference on Power Electronics (IICPE)*, Dec. 2018, pp. 1–6, doi: 10.1109/IICPE.2018.8709425.

[29] M. Ergin Şahin, "A photovoltaic powered electrolysis converter system with maximum power point tracking control," *International Journal of Hydrogen Energy*, vol. 45, no. 16, pp. 9293–9304, Mar. 2020, doi: 10.1016/j.ijhydene.2020.01.162.

[30] A. Haque and Zaheeruddin, "A fast and reliable perturb and observe maximum power point tracker for solar PV system," *International Journal of System Assurance Engineering and Management*, vol. 8, no. S2, pp. 773–787, Nov. 2017, doi: 10.1007/s13198-016-0523-2.

[31] M. S. Ebrahim, A. M. Sharaf, A. M. Atallah, and A. S. Emarah, "Modified P&O technique for hybrid PV-battery smart grid integrated scheme," *Turkish Journal of Electromechanics & Energy*, vol. 3, no. 2, pp. 1–7, 2018.

[32] R. Bhukya and N. Shanmugasundaram, "Performance investigation on novel MPPT controller in solar photovoltaic system," *Materials Today: Proceedings*, vol. 80, pp. 3517–3522, 2023, doi: 10.1016/j.matpr.2021.07.286.

[33] M. Abdel-Nasser, K. Mahmoud, and M. Lehtonen, "Reliable solar irradiance forecasting approach based on choquet integral and deep LSTMs," *IEEE Transactions on Industrial Informatics*, vol. 17, no. 3, pp. 1873–1881, Mar. 2021, doi: 10.1109/TII.2020.2996235.

[34] T. Yu *et al.*, "Photovoltaic panel temperature monitoring and prediction by raman distributed temperature sensor with fuzzy temperature difference threshold method," *IEEE Sensors Journal*, vol. 21, no. 1, pp. 373–380, Jan. 2021, doi: 10.1109/JSEN.2020.3015508.

[35] O. Kraa *et al.*, "States feedback control applied to the electric vehicle," *Energy Procedia*, vol. 50, pp. 186–193, 2014, doi: 10.1016/j.egypro.2014.06.023.

[36] M. Habib, F. Khoucha, and A. Harrag, "GA-based robust LQR controller for interleaved boost DC–DC converter improving fuel cell voltage regulation," *Electric Power Systems Research*, vol. 152, pp. 438–456, Nov. 2017, doi: 10.1016/j.epsr.2017.08.004.

[37] Y. Zhi, W. Weiqing, H. Shan, and S. Mizzi, "Interval-based LQR strategy for optimal control of proton exchange membrane fuel cell system with interval uncertainties," *ISA Transactions*, vol. 100, pp. 334–345, May 2020, doi: 10.1016/j.isatra.2019.11.016.

[38] A. S. Elkhatem and S. N. Engin, "Robust LQR and LQR-PI control strategies based on adaptive weighting matrix selection for a UAV position and attitude tracking control," *Alexandria Engineering Journal*, vol. 61, no. 8, pp. 6275–6292, Aug. 2022, doi: 10.1016/j.aej.2021.11.057.

BIOGRAPHIES OF AUTHORS

Mohamed Assabaa received the engineer degree in electronics (systems control) from University of Constantine 1, Algeria, in 2002 and the magister and doctorate degrees in electronics (systems control) in 2006 and 2015, respectively, from the Department of Electronics, University of Constantine 1, Algeria. Currently, he is an associate professor in the Electromechanical Department at the Institute of Sciences and Applied Techniques, University of Constantine 1, Algeria. His research interests include fractional-order control, adaptive control, robust control, fractional-order systems, renewable energy, and industrial automation. He can be contacted at: mohamed.assabaa@umc.edu.dz or assabaamohamed@gmail.com.

Adel Bouchahed was born in Guelma, Algeria, on April 10, 1980. Higher education was completed in Heliopolis City, Algeria, graduating with a bachelor's degree in electrotechnics in 2000. Postgraduate diplomas in electromechanical engineering were received from Annaba University in 2006. The electromechanical magister degree was received from Annaba University in 2009. The electromechanical doctorate degree was received in 2017 from Annaba University. He is an associate professor at the Institute of Sciences and Applied Techniques, University of Constantine 1. His present research interests include electrical vehicles, renewable energy, power electronics, and industrial automation. He can be contacted at email: bouchahed.adel@umc.edu.dz or adel.bouchahed@gmail.com.

Abdellah Draidi received the engineer degree in electrotechnics from University of Constantine 1, Algeria, in 2006 and the magister and doctorate degrees in electrotechnics in 2010 and 2016, respectively, from the Department of Electrotechnics, University of Constantine 1, Algeria. Currently, he is an associate professor and head of the Electromechanical Department at the Institute of Sciences and Applied Techniques (Institut des Sciences et Techniques Appliquées, ISTA), University of Constantine 1, Algeria. His research interests include renewable energy, power systems, load flow control, economic dispatch, artificial intelligence techniques, and industrial automation. He can be contacted at email: draidi_abdellh@umc.edu.dz or abdellah.draidi@gmail.com.

Boudjema Mehimmedetsi received the electromechanical engineer degree from University of Annaba, Algeria, in 1992 and the magister and doctorate degrees in electrotechnics in 2008 and 2018, respectively, from the Department of Electrotechnics, University of Constantine 1, Algeria. Currently, he is an associate professor at the Electromechanical Department, University of Mila, Algeria. His research interests include renewable energy, power systems, hybrid power systems, and control of electrical machines. He can be contacted at email: mehim.boudj@gmail.com or b.mehimmedetsi@centre-univ-mila.dz.

Ahmed Belhani has received an engineer degree, master's degree, and Ph.D. degree in control engineering from the University of Constantine 1, Algeria. Currently, he is a full professor in the Electronics Department, Faculty of Science and Technology, University of Constantine 1. His research interests include nonlinear control, artificial intelligence (AI), renewable energy, hybrid systems, optimization, FPGA, and embedded systems. He can be contacted at email: ahmed.belhani@umc.edu.dz.